

# Reduction of Climate Sensitivity to Solar Forcing due to Stratospheric Ozone Feedback

G. CHIODO

*Department of Applied Physics and Applied Mathematics,  
Columbia University, New York, New York*

L. M. POLVANI

*Department of Applied Physics and Applied Mathematics, Department of Earth  
and Environmental Sciences, and Lamont-Doherty Earth Observatory,  
Columbia University, New York, New York*

(Manuscript received 7 October 2015, in final form 5 February 2016)

## ABSTRACT

An accurate assessment of the role of solar variability is a key step toward a proper quantification of natural and anthropogenic climate change. To this end, climate models have been extensively used to quantify the solar contribution to climate variability. However, owing to the large computational cost, the bulk of modeling studies to date have been performed without interactive stratospheric photochemistry: the impact of this simplification on the modeled climate system response to solar forcing remains largely unknown. Here this impact is quantified by comparing the response of two model configurations, with and without interactive ozone chemistry. Using long integrations, robust surface temperature and precipitation responses to an idealized irradiance increase are obtained. Then, it is shown that the inclusion of interactive stratospheric chemistry significantly reduces the surface warming (by about one-third) and the accompanying precipitation response. This behavior is linked to photochemically induced stratospheric ozone changes, and their modulation of the surface solar radiation. The results herein suggest that neglecting stratospheric photochemistry leads to a sizable overestimate of the surface response to changes in solar irradiance. This has implications for simulations of the climate in the last millennium and geoengineering applications employing irradiance changes larger than those observed over the 11-yr sunspot cycle, where models often use simplified treatments of stratospheric ozone that are inconsistent with the imposed solar forcing.

## 1. Introduction

Variations in solar activity exert a strong influence on the upper atmosphere: however, their effects on tropospheric and surface climate are still only partly understood (Gray et al. 2010). Over the 11-yr sunspot cycle, the relatively weak amplitude of the solar forcing change ( $\sim 0.17 \text{ W m}^{-2}$ ) and its nonstationarity limit the emergence of a robust surface signal. On the other hand, century-scale variations in total solar irradiance (TSI) may have been larger than those recorded over the 11-yr cycle, as suggested by proxy-based reconstructions

(Fröhlich and Lean 2004), although the amplitude of these changes in solar forcing is highly uncertain. In this context, climate models are a fundamental tool to characterize the tropospheric and surface climate response to solar irradiance changes and, more generally, to quantify the climate sensitivity to solar forcing. This question is of fundamental interest in attribution studies, which are aimed at assessing the role of solar forcing in driving climate variability and climate change.

It is well established that the ozone–UV feedback plays a dominant role in amplifying the thermal response to 11-yr solar variability (Haigh 1994, 1996; Shindell et al. 1999). To capture this feedback in climate models, an interactive stratospheric ozone chemistry is essential (Haigh 1994; Gray et al. 2010). Given that the stratosphere is a key component in the top-down propagation of the 11-yr solar signal to the surface (Meehl et al. 2009), it would

---

*Corresponding author address:* G. Chiodo, Department of Applied Physics and Applied Mathematics, 200 Seeley W. Mudd Building, 2nd floor, 500 West 120th Street, New York, NY 10027.  
E-mail: chiodo@columbia.edu

follow that an interactive stratospheric chemistry could be an important ingredient to accurately model the climate system response to solar forcing. However, because of computational constraints, this component is commonly neglected in many Earth system models employed in intercomparison projects, such as the Paleoclimate Intercomparison Project (PMIP) (Hegerl et al. 2011; Fernández-Donado et al. 2013) and phase 5 of the Coupled Model Intercomparison Project (CMIP5) (Eyring et al. 2013). This is also the case in many of the models employed in geoengineering (GeoMIP) studies until recently (H. Schmidt et al. 2012; Tilmes et al. 2013; Huneus et al. 2014), aimed at quantifying the efficiency of solar radiation management approaches.

Including interactive chemistry, and consequently interactive ozone, is one of the current strategies in climate model development (Eyring et al. 2010; Myhre et al. 2014). In the last decade, the importance of stratospheric ozone changes on the climate of the Southern Hemisphere has been widely recognized [see the recent reviews of Thompson et al. (2011) and Previdi and Polvani (2014)]. More recently, the impact of interactive stratospheric chemistry on climate sensitivity has been quantified (Dietmüller et al. 2014; Nowack et al. 2014). These studies have consistently shown that including interactive stratospheric chemistry reduces the surface response to a quadrupling of CO<sub>2</sub> concentrations. The aim of this paper is to examine whether a similar effect exists in the case of solar forcing.

Neglecting the ozone photochemistry can be potentially detrimental for the modeled stratospheric response to solar forcing, due to the absence of the ozone–UV feedback; however, it is unknown whether, and to what extent, the modeled tropospheric and surface response are also affected (Gray et al. 2010). In the present work, we provide answers to this question by carrying out model simulations from the Community Earth System Model (CESM), using the stratosphere-resolving Whole Atmosphere Community Climate Model (WACCM), and different configurations for the stratospheric chemistry. In its latest version, WACCM easily allows coupling and decoupling of stratospheric ozone chemistry without altering *any* of the model components or parameterizations (Smith et al. 2014). This makes WACCM ideally suited for the present study, as changes in the modeled response to solar forcing can be unambiguously attributed to the chemistry coupling.

## 2. Methods

### a. Model setup

We use the Community Earth System Model (Marsh et al. 2013), a global climate model whose atmospheric

component is the Whole Atmosphere Community Climate Model version 4, coupled to the Parallel Ocean Program (POP) ocean circulation model (Gent et al. 2011). The resolution in WACCM is 1.9° latitude and 2.5° longitude with 66 vertical levels with an upper boundary at 140 km, providing a well-resolved middle atmosphere. The standard configuration of WACCM includes a fully interactive stratospheric chemistry module, based on the version 3 of the Model for Ozone and Related Chemical Tracers (MOZART; Kinnison et al. 2007), which calculates 217 gas-phase chemical reaction and advects a total of 59 species. Photolysis rates are calculated in-line using a resolution of 66 bands, covering all absorption lines from 120 nm onward [details of the photochemistry calculations are given in Marsh et al. (2007)]. Most importantly, the impact of solar variability is treated in a self-consistent way in the chemistry and radiation schemes, since the same solar spectral irradiance (SSI) forcing is used as input for both photolysis and heating rate calculations. This leads to a realistic representation of the shortwave (SW) heating in the stratosphere and, consequently, of the atmospheric response to solar forcing perturbations (Chiodo et al. 2012).

In this paper, we also take advantage of an alternative configuration of the CESM model, which uses, as its atmospheric component, the Specified Chemistry Whole Atmosphere Community Climate Model (SC-WACCM). SC-WACCM inherits all physics and radiation packages from WACCM and uses an identical grid space (i.e., a high resolution in the middle atmosphere) but does not include the MOZART-3 chemistry module. Instead, the concentrations of radiatively active gases such as O<sub>3</sub>, NO, O, O<sub>2</sub>, and CO<sub>2</sub> are simply specified throughout the atmospheric domain, using zonal mean values obtained from a 300-yr-long WACCM preindustrial control simulation (this includes a seasonal cycle). Since chemical heating is not parameterized in SC-WACCM (due to the absence of interactive chemistry), SW heating rates are prescribed in the mesosphere and lower thermosphere (MLT) region to ensure the total energy input is nearly identical to WACCM. This leads to small biases in the MLT region, but these do not affect the basic state in the lower levels (Smith et al. 2014).

### b. Experiment design

To quantify the role of chemistry coupling on the climate response to solar forcing, we have performed a set of 300-yr-long integrations (see Table 1). To avoid drifts, initial conditions were obtained from a previously well spun-up WACCM integration. Then, a preindustrial control integration using these initial conditions was carried out using WACCM (denoted ctrl), with interactive stratospheric chemistry and constant spectral solar

TABLE 1. The WACCM model integrations analyzed in this study. All integrations are 300 yr long, with time-independent solar forcing. The ctrl integration is at preindustrial values, and invokes an interactive chemistry; ctrl4W is the corresponding perturbed integration, with the SSI forcing increase by  $4 \text{ W m}^{-2}$ . For the pair without interactive chemistry, ctrl\_nochem and ctrl4W\_nochem, the ozone is specified (with an annual cycle) from the time mean of the ctrl integration. The ctrl4W\_nochem\_o3 integration is identical to ctrl4W\_nochem except that the ozone is specified from the ctrl4W integration. All experiments are performed with coupled land, ocean, and sea ice components.

Name	Solar	Ozone	Years
ctrl	SSI = $1361 \text{ W m}^{-2}$	interactive	300
ctrl4W	SSI = $1365 \text{ W m}^{-2}$	interactive	300
ctrl_nochem	SSI = $1361 \text{ W m}^{-2}$	ctrl	300
ctrl4W_nochem	SSI = $1365 \text{ W m}^{-2}$	ctrl	300
ctrl4W_nochem_o3	SSI = $1365 \text{ W m}^{-2}$	ctrl4W	300

irradiance (SSI) of  $1361 \text{ W m}^{-2}$ . Then, we carried out one perturbed integration with the same model (denoted ctrl4W), but with an increase of  $4 \text{ W m}^{-2}$  (or 0.29%) in SSI forcing. The difference of these integrations allows us to establish a clear surface response to the imposed solar forcing. Next, a similar pair of integrations was performed, but *without* interactive stratospheric chemistry using SC-WACCM (denoted ctrl\_nochem and ctrl4W\_nochem, respectively), in which we specified zonal-mean, monthly-mean ozone values according to the 300-yr mean climatology from the WACCM control run (ctrl). Thus, their difference (ctrl\_nochem – ctrl4W\_nochem) allows us to establish the response to solar forcing in the absence of ozone changes.

It has been previously shown that under preindustrial boundary conditions, equivalent to those employed in the ctrl and ctrl\_nochem experiments, the climatology and variability of stratospheric, tropospheric, and surface climate in SC-WACCM and WACCM are nearly identical (Smith et al. 2014). Therefore, comparing the pairs of integrations allows us to quantify the relative importance of interactive chemistry on the simulated response, which is the key purpose of the present paper. In addition, to gain conclusive evidence as to the role of ozone in modulating the surface response, we also carried out one integration with SC-WACCM, in which we specified the ozone field simulated by the forced WACCM run (ctrl4W\_nochem\_o3).

### c. Solar spectral irradiance forcing

The spectral dependency of the SSI changes imposed in the perturbed runs is taken from the Naval Research Laboratory Solar Spectral Irradiance semiempirical model (NRL-SSI; see Wang et al. 2005) and is consistent

with that observed during peaks of the 11-yr sunspot cycle in this dataset, albeit scaled by a factor of 4, for the purpose of producing a strong surface climate response. Accordingly, the relative increase in the UV (200–350 nm) is larger than in the visible range (351–700 nm), with a 7%–40% ( $0.93 \text{ W m}^{-2}$ ) change in the former, and 0.4% change ( $2.1 \text{ W m}^{-2}$ ) in the latter. Our idealized UV forcing is larger than in most semiempirical models, but smaller than the 11-yr solar cycle variability seen in recent Solar Radiation and Climate Experiment (SORCE)-Spectral Irradiance Monitor (SIM) satellite data (Ermolli et al. 2013). In addition, the imposed SSI forcing does not contain the compensating trends between visible and ultraviolet changes observed over the descending phase of solar cycle 23 in SORCE-SIM (Harder et al. 2009).

The solar forcing changes imposed in the perturbed cases are larger than the 11-yr solar cycle (by a factor of 4); however, they are near the upper end of the range of reconstructed estimates over the last millennium (G. Schmidt et al. 2012) and therefore not entirely unrealistic in the context of centennial-scale solar variability and geoengineering studies employing larger irradiance reductions [see, e.g., Table 2 in H. Schmidt et al. (2012)]. The underlying assumption is that SSI variations that are larger than 11-yr solar cycle will exhibit the same shape as those observed in the NRL-SSI data over the 11-yr sunspot cycle. Because of the idealized amplitude of our SSI forcing, it is possible that the results obtained may not be representative for the 11-yr solar cycle. However, the response to the 11-yr solar cycle is most pronounced regionally (e.g., Ineson et al. 2011; Meehl et al. 2009; Chiodo et al. 2012) and therefore it is not useful to quantify the “climate sensitivity” to solar forcing, which is the primary purpose of this paper. This is accomplished by 1) prescribing a relatively large and steady forcing and 2) performing long integrations to equilibrium: the first amplifies the signal, the second reduces the noise. This is a common approach when establishing the climate sensitivity to well-mixed greenhouse gases (GHG), where an instantaneous quadrupling of  $\text{CO}_2$  is typically applied (e.g., Nowack et al. 2014), although such forcing is not immediately comparable to any observations.

### d. Statistical method

Throughout this paper, we assess the statistical significance of the differences using a Student’s *t* test for climatologies, and a Kolmogorov–Smirnov (K-S) test for probability density functions (PDFs), which are computed with a kernel density estimator. The null hypothesis is that differences in the climatological averages are not different from zero, and that PDFs are not different from each other. Differences

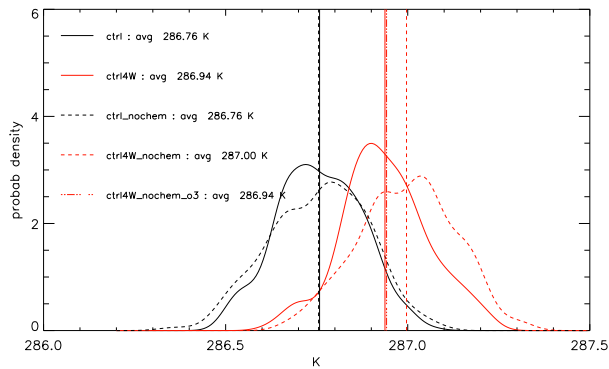


FIG. 1. Probability density distribution of global mean surface air temperature (SAT) from the 300-yr-long control integrations using the coupled and specified chemistry configurations. The black lines show the output from the control integrations using a SSI value close to the recent solar cycle minima ( $1361 \text{ W m}^{-2}$ ); the perturbed runs forced with a spectrally resolved SSI increase of  $4 \text{ W m}^{-2}$  are depicted in red. Solid lines indicate the coupled chemistry integrations; dashed lines the specified chemistry ones. The numbers and vertical lines indicate the long-term averages in units K. The dash-dotted line shows the global mean long-term average obtained from an integration using the specified chemistry model forced with an increased SSI, and the ozone response from the coupled chemistry integration.

are considered significant when they exceed the 0.05 (95%) confidence level.

### 3. Climate response to solar spectral irradiance with and without coupled chemistry

#### a. Surface response

We start by examining the PDFs of the annual mean surface air temperature (SAT), constructed from the 300-yr-long model integrations. Consider first the solid lines in Fig. 1, which illustrate the model integrations with interactive chemistry: the control case and the perturbed case are well separated, indicating a statistically significant surface response accompanying an increase in solar irradiance. The global mean difference in surface air temperature ( $\delta\text{SAT}$ ) between these two integrations is 0.18 K, implying a sensitivity parameter of  $0.24 \text{ K (W m}^{-2})^{-1}$ . For comparison, the canonical equilibrium sensitivity parameter in WACCM, measured as a  $\delta\text{SAT}$  response to a doubling in  $\text{CO}_2$ , is  $0.72 \text{ K (W m}^{-2})^{-1}$  (D. Marsh 2015, personal communication), in line with other CMIP5 models (Sherwood et al. 2014). Therefore, the SSI forcing has a relatively low “efficacy” compared to  $\text{CO}_2$ , which is consistent with previous work (Hansen et al. 2005).

In the absence of ozone changes, the difference between the control and perturbed integrations is also statistically significant, but considerably larger than that in the interactive

chemistry integrations, with a  $\delta\text{SAT} = 0.24 \text{ K}$ , corresponding to a sensitivity parameter of  $0.32 \text{ K (W m}^{-2})^{-1}$ . This is the key result of our study: without ozone changes the global mean surface temperature response is roughly 35% larger than in the case with interactive stratospheric chemistry. We have established the robustness of this result by verifying that the PDFs of the two integrations with increased solar irradiance (red lines in Fig. 1) are statistically different at the 99% level, according to the K-S test (the control integrations with and without interactive stratospheric chemistry—the black lines—are statistically indistinguishable).

The amplification of the surface response in the absence of interactive chemistry is quite rapid, and does not require centennial scales to emerge. The response difference between the interactive and specified chemistry cases is already present after a few decades of integration, even though the models are not entirely equilibrated to the initial forcing. Hence, the inclusion of interactive ozone chemistry reduces not only the steady-state response (or equilibrium climate sensitivity) but also the transient climate response to solar forcing.

The forcing/sensitivity perspective gives only a very partial picture of the climate response to the imposed increase in solar irradiance. To gain more insights one needs to explore the regional patterns of the SAT response; these are shown in Figs. 2a and 2b for the interactive and prescribed chemistry integrations. A surface warming is clearly visible in both cases, with slightly larger amplitude over the continents than over the ocean, and a polar amplification in the Northern Hemisphere. This response pattern is quite similar to the one caused by increased GHG [see, e.g., Fig. 12.11 in Myhre et al. (2014)] and to the response to solar forcing reported in simpler models (Wetherald and Manabe 1975; Cubasch et al. 1997; Ammann et al. 2007). However, the surface warming in the absence of interactive chemistry is considerably more pronounced than in the coupled chemistry case, especially over the continents and in the northern high latitudes.

The surface temperature difference between the two configurations is more evident in the zonal mean (Fig. 3), which shows less warming in the presence of interactive chemistry at all latitudes, but especially at northern high latitudes, where the difference between interactive and specified chemistry can be a factor of 2. Clearly, the inclusion of interactive chemistry leads to a sizable reduction of the climate sensitivity to solar forcing, and that reduction can locally be of the same magnitude as the response itself, for instance over the Arctic.

Together with reduced surface warming, our experiments also show a reduction in tropical precipitation

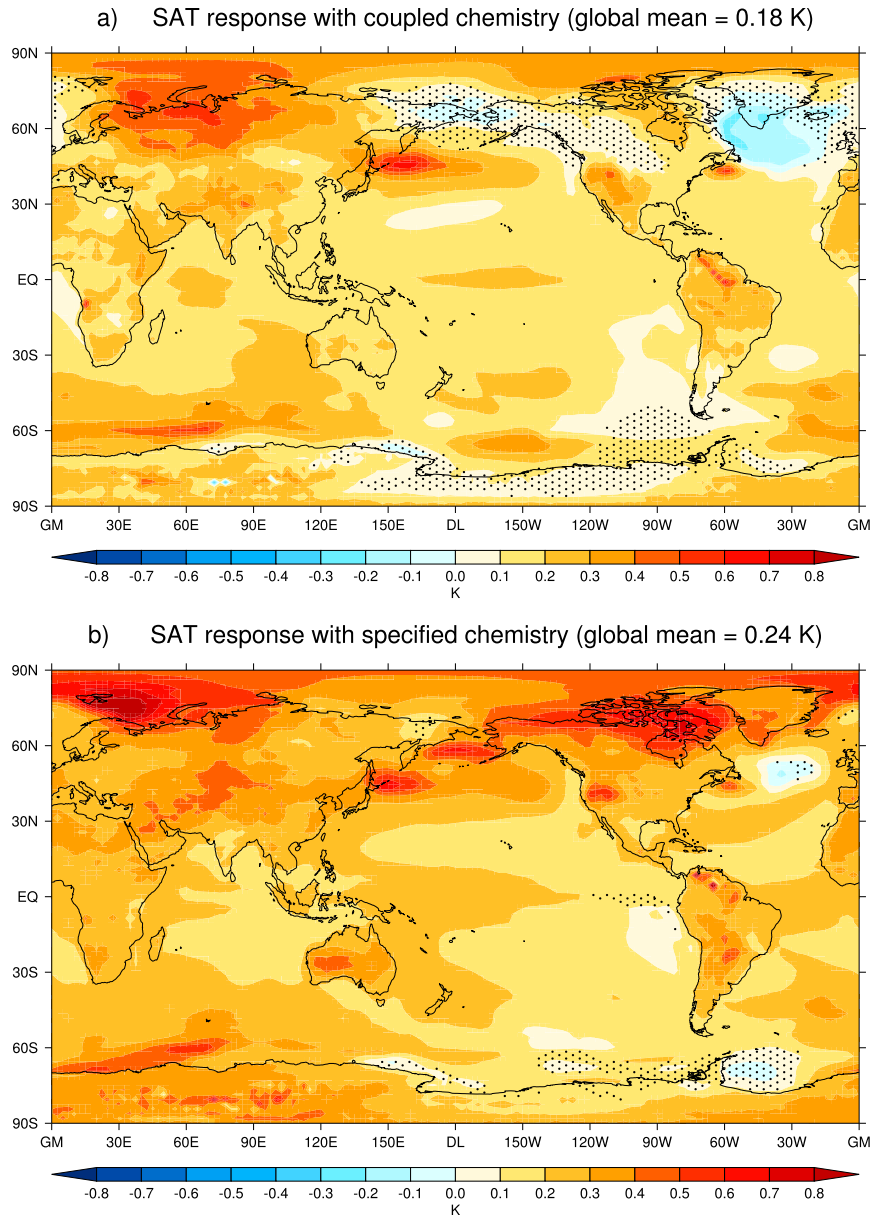


FIG. 2. SAT response from the (a) coupled and (b) specified chemistry configuration, quantified as (ctrl4W – ctrl) and (ctrl4W\_nochem – ctrl\_nochem) differences, respectively. Dotted areas denote differences that are not statistically significant at the 95% confidence level. Units: K.

signals, notably over the warm pool region (Fig. 4), in the integrations with interactive stratospheric chemistry. The patterns of precipitation response in our integrations, with either configuration of the model chemistry, are in good agreement with those reported for the peaks of the 11-yr cycle (Meehl et al. 2003; Shindell et al. 2006; Meehl et al. 2008). However, the response is significantly smaller in the integrations with coupled chemistry (Fig. 4a), and the differences

between coupled and uncoupled chemistry can locally be as large as 100%.

To understand the dynamical component of the precipitation response, we investigate the changes in the tropical Pacific circulation, shown in Fig. 5. Climatologically, one finds the familiar clockwise circulation over the Pacific Ocean, commonly referred to as the Walker cell. With increased SSI, a strengthening of the Walker circulation occurs in both coupled and specified

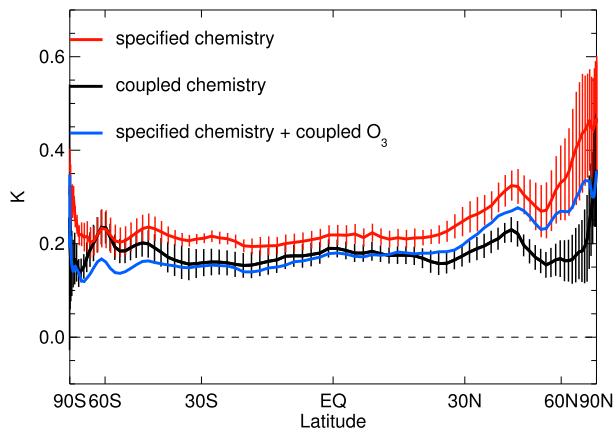


FIG. 3. Zonal mean SAT response in the coupled (black) and specified chemistry run (red). Error bars represent the  $1\text{-}\sigma$  uncertainty in 30-yr-long overlapping segments. The blue line shows the response in the specified chemistry case forced with the ozone response to increased SSI calculated with interactive chemistry (denoted `ctrl4W_nochem_o3`). Units: K.

chemistry cases, so that the precipitation response is closely tied to a strengthening in the Walker circulation, in agreement with the previously reported response to peaks in solar activity (Meehl et al. 2003; Lee et al. 2009). The novelty here is that the strengthening of the Walker circulation with interactive chemistry is considerably smaller than with specified chemistry.

Globally, a precipitation increase of  $0.019\text{ mm day}^{-1}$  is obtained in the specified chemistry case, which reduces to only  $0.009\text{ mm day}^{-1}$  when an interactive chemistry is used. By using a simple linear scaling with the SAT response shown in Fig. 1 (see Andrews et al. 2010), we obtain a hydrological sensitivity  $\delta P/\delta\text{SAT}$  of  $2.8\% \text{ K}^{-1}$  in the specified chemistry integration, which is close to the  $2.5\% \text{ K}^{-1}$  response to solar forcing obtained in another model with specified chemistry (HadGEM1) (Andrews et al. 2010). More importantly, the hydrological sensitivity is reduced to  $1.7\% \text{ K}^{-1}$  in the interactive chemistry case: a reduction of 40%. While the chemistry coupling significantly reduces both temperature and precipitation responses to solar forcing, the changes in the latter are slightly more pronounced, possibly owing to the intrinsically strong sensitivity of the hydrological cycle to solar forcing, as compared to other forcings, such as  $\text{CO}_2$  (Kleidon and Renner 2013).

### b. Zonal mean temperature and ozone response

To understand the mechanism behind such striking differences in the climate sensitivity, we now turn our attention to the vertical structure of the response. The zonal mean temperature response, as a function of latitude and height, is shown for the interactive (Fig. 6a) and

specified (Fig. 6b) chemistry configurations. As one would expect, the increase in SSI leads to a warming of the stratosphere, which increases monotonically with height, reaching 3 K in the upper stratosphere around 50 km in the coupled chemistry experiment (Fig. 6a). A similar vertical structure is also present in the specified chemistry integration (Fig. 6b). However, a weaker stratospheric warming and a more prominent tropical upper tropospheric warming are apparent. To bring out the differences between the coupled and uncoupled chemistry responses, we plot their difference in Fig. 6c. First, it is clear that the interactive chemistry causes an enhanced heating of the stratosphere, as it has been previously reported (Haigh 1996). The color scale in Fig. 6c is identical to the one in Figs. 6a and 6b, indicating that the differences due to interactive chemistry are comparable to the response itself. Second, and this is the key finding of this work, the interactive stratospheric chemistry causes a reduced warming in the troposphere and the surface (which appears as a cooling below the tropopause in Fig. 4c).

To understand these temperature differences between the coupled and uncoupled chemistry integrations, we now turn to the ozone response. Since ozone concentrations do not change with increased SSI unless the chemistry is interactive, we only need to consider the ozone response in the coupled chemistry integrations; this response (in percentage) is illustrated in Fig. 6d. With stronger SSI forcing, ozone increases throughout the troposphere and the stratosphere, with three distinct maxima in the stratosphere: two are found in the mid-stratosphere (around 30 to 40 km) at middle to high latitudes, and the third is located in the tropical lower stratosphere (around 20 km). The former are due to UV-induced enhanced oxygen photolysis, while the latter is due to a weakening in tropical upwelling (not shown). Overall, the structure of the stratospheric ozone response in Fig. 6d is in agreement with that observed by the SAGE instrument during peaks of solar activity (Soukharev and Hood 2006; Randel and Wu 2007), indicating a realistic photochemical response in WACCM. The ozone response in Fig. 6d also resembles the one found in WACCM in response to the 11-yr solar cycle (Chiodo et al. 2012; Peck et al. 2015), but with a fourfold larger amplitude in the present integrations than those for the 11-yr cycle, consistent with the larger UV input.

In contrast to the results reported in Haigh et al. (2010), we do not obtain a vertical dipole in the response of ozone to solar forcing, with a decrease in the upper stratosphere and an increase in the midstratosphere. This difference might be due to the use of a weaker UV forcing, as compared to the SORCE-SIM data employed in Haigh et al. (2010). Imposing a larger UV forcing would lead to ozone decrease in upper stratospheric levels, and an

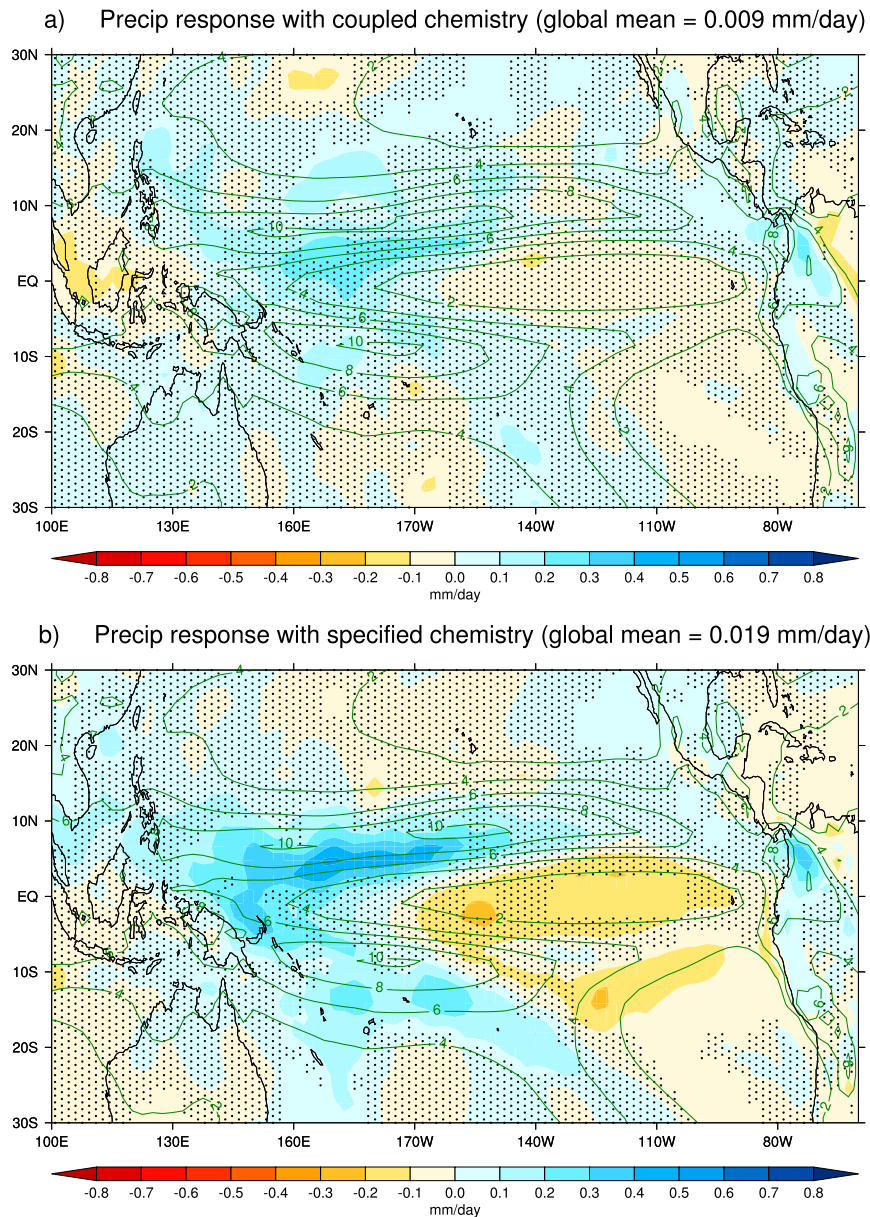


FIG. 4. As in Fig. 2, for total precipitation in the tropical Pacific. The green contour lines represent the climatological precipitation values. Units:  $\text{mm day}^{-1}$ .

ozone increase at lower stratospheric levels. Overall, this can be viewed as a downward shift in the peak response to the middle-lower stratosphere, as shown by [Merkel et al. \(2011\)](#). Accordingly, the vertical structure of the ozone response is a nonlinear function of the size of the UV forcing, which is due to the contribution of UV to both photolytic ozone destruction and recombination, as suggested by [Haigh et al. \(2010\)](#). Nevertheless, a downward shift of the ozone response with increasing UV forcing would result in a larger column-integrated ozone perturbation, implying that the change in total ozone will

scale with the UV forcing. Clearly, more sensitivity experiments are needed to elucidate this.

From the ozone response to increased SSI, it is easy to understand the larger stratospheric temperature response in the interactive chemistry experiment: it simply results from the additional shortwave absorption due to the (UV-induced) ozone increase, as indicated by an increase in stratospheric SW heating rates (not shown), and the upward shift in the maximum heating with respect to the ozone response in the upper stratosphere. The tropospheric temperature difference, however, is not

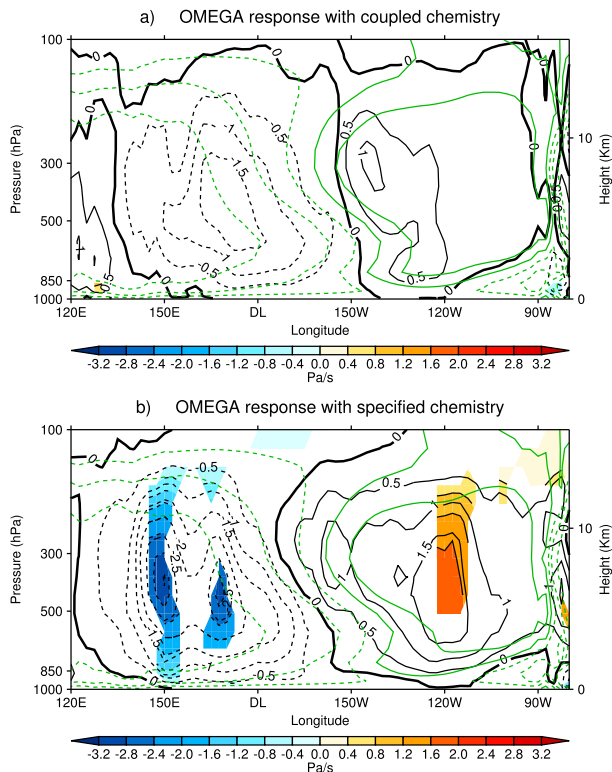


FIG. 5. Meridionally averaged tropical mean ( $5^{\circ}\text{N}$ – $10^{\circ}\text{S}$ ) vertical velocity ( $\omega$ ) response in the Pacific sector in the (a) coupled and (b) specified chemistry configuration. The overlaid green lines show the climatology; solid (dashed) lines indicate positive (negative) values. Negative values denote ascent, positive values descent. Colored areas identify differences that are statistically significant at the 95% confidence level. Units:  $\text{Pa s}^{-1}$ .

immediately obvious. To show that ozone is key to explaining the difference in the tropospheric and surface response, we have performed an additional perturbed integration, with the noninteractive chemistry model configuration (denoted `ctrl4W_nochem_o3`), but in which we have specified the ozone climatology computed from the perturbed run with coupled chemistry (`ctrl4W`), in addition to an increased SSI (see Table 1). This means that the solar-induced increase in ozone shown in Fig. 6d is imposed.

As one can see in Fig. 1 (vertical dashed-dotted red line), this integration reproduces the global mean SAT changes of the coupled chemistry integration with remarkable accuracy (yielding an identical  $\delta\text{SAT}$  of 0.18 K), proving a clear link between the increase in stratospheric ozone and the reduced long-term global mean surface response in the presence of interactive chemistry. We note some regional differences between the `ctrl4W` and `ctrl4W_nochem_o3` runs, mostly in the northern high latitudes (see Fig. 3; compare the dashed light blue and solid black lines), possibly due to the fact that monthly mean, zonal mean ozone climatological

values are used in the specified chemistry configuration; these simplifications are known to cause inaccuracies in the surface response to stratospheric ozone perturbations (Gillett et al. 2009; Waugh et al. 2009; Neely et al. 2014), but they are not sufficiently severe to affect the global mean temperature response.

There is also an ozone increase in the lower troposphere in Fig. 6d, which is related to an increase in  $\text{NO}_x$  emission from enhanced lightning activity, associated with convection in the tropics. First, recall that those are percentage changes, and tropospheric ozone concentrations are small compared to those in the stratosphere. Second, to separate the role of stratospheric and tropospheric ozone, we performed an additional model integration using only the stratospheric portion (i.e., above 100 hPa) of the ozone response depicted in Fig. 6d. This integration yields a global mean  $\delta\text{SAT}$  of 0.19 K, which is very close to the  $\delta\text{SAT}$  of 0.18 K found in the `ctrl4W_nochem_o3` case. From this, we safely conclude that the difference in the surface response between the coupled and specified chemistry integrations is almost entirely due to stratospheric ozone changes.

### c. Mechanism

Finally, we elucidate the mechanism that allows stratospheric ozone to alter the surface response to SSI changes. In a nutshell, the increased SSI leads to a photolytically induced increase in stratospheric ozone. Increased stratospheric ozone absorbs more SW radiation in the Hartley–Huggins UV (200–300 nm) and Chappuis visible (450–600 nm) bands (Goody and Yung 1989). While the former absorption bands are responsible for the enhanced stratospheric heating, the latter reduce the visible portion of solar radiation, which ultimately affects the surface energy balance, reducing the surface warming. This is why the model sensitivity is smaller with interactive chemistry than without. The effect of coupled ozone chemistry is clearly seen in the zonal mean clear-sky downwelling SW flux at the surface, shown in Fig. 7a. This field captures the energy absorbed in subtropical oceanic cloud-free areas, and plays a key role in initiating the “bottom-up” mechanism (e.g., White et al. 1997; Meehl et al. 2009).

In the specified chemistry case (i.e., with ozone fixed; red curve) the SSI increase at the top of the atmosphere (TOA) translates into an increase in clear-sky downwelling SW flux, peaking at  $0.5 \text{ W m}^{-2}$  at low latitudes and tapering gradually to  $0.2 \text{ W m}^{-2}$  in high latitudes; that increase is considerably reduced, at all latitudes, in the coupled chemistry case (black curve). When cloud adjustments are taken into account (Fig. 7b), a net positive surface SW flux of  $0.3$ – $0.5 \text{ W m}^{-2}$  is still present in the specified chemistry run; however, in the coupled

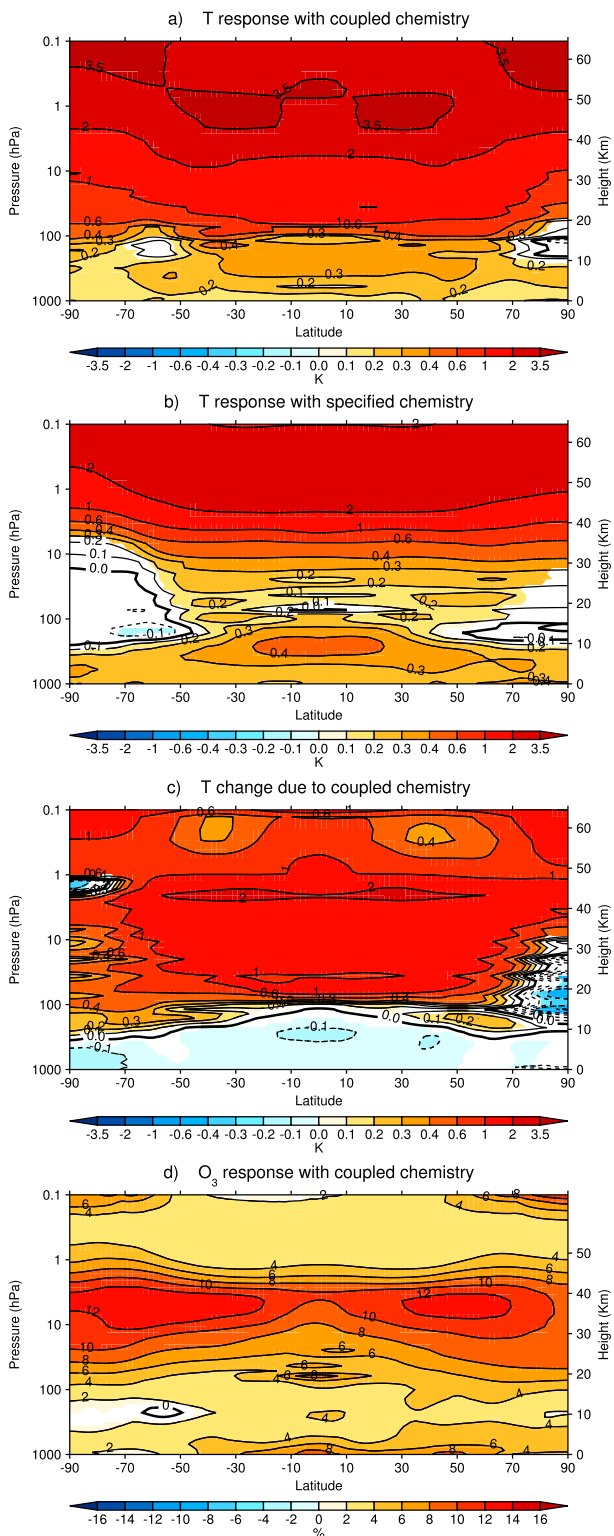


FIG. 6. Zonal mean temperature response from the coupled (a) and specified (b) chemistry integration. (c) Contribution of the chemistry coupling to the response, quantified as the difference between perturbed runs (ctrl4W – ctrl4W\_nochem). (d) Relative (%) zonal mean ozone response from the coupled chemistry integration. Colored areas denote statistically significant differences at the 95% confidence level.

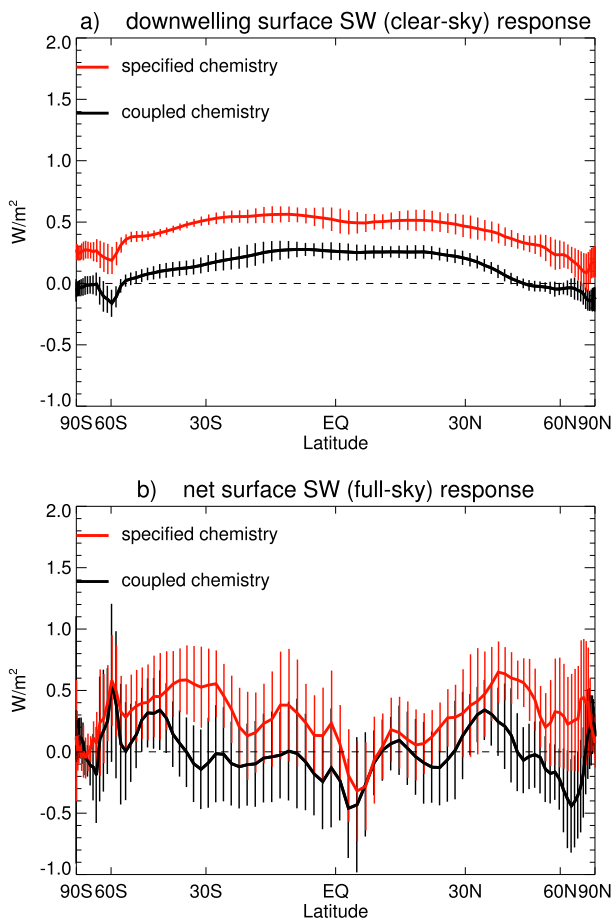


FIG. 7. (a) Response of the zonal mean clear-sky downwelling surface SW flux in the coupled (black) and specified chemistry cases (red). (b) As in (a), but for the net surface SW flux (full sky). Units:  $W m^{-2}$ .

chemistry case a net positive surface SW budget is only found at midlatitudes. Globally, the coupled chemistry run shows a reduction in the surface SW flux of  $\sim 0.3 W m^{-2}$  relative to the specified chemistry integration.

One might wonder if stratospheric ozone directly affects the SW radiation budget, or whether atmospheric feedbacks might be present (e.g., through changes in water vapor or cloud cover). To address that question, we performed offline calculations using the Parallel Offline Radiative Transfer (PORT) model (Conley et al. 2012), using the same SSI forcing employed in the control (port) and perturbed (port4W) runs, but keeping all radiatively active gases, including ozone, fixed. Comparing the atmospheric SW absorption (quantified as difference between SW fluxes at TOA and surface) in the offline PORT and free-running WACCM integrations (see Table 2), it is possible to separate forcing and feedbacks. With increased SSI, PORT shows an increase in SW

TABLE 2. Global long-term mean change between perturbed and control experiments in SW fluxes at TOA, and atmospheric absorption. Units:  $\text{W m}^{-2}$ .

	$\delta\text{SW}_{\text{toa}}$	$\delta\text{abs}$
ctrl4W – ctrl	0.95	0.71
ctrl4W_nochem – ctrl_nochem	0.75	0.40
port4W – port	0.76	0.39

fluxes at TOA ( $0.76 \text{ W m}^{-2}$ ) and in atmospheric absorption ( $0.39 \text{ W m}^{-2}$ ), values that are close to those obtained in the specified chemistry case ( $0.71$  and  $0.40 \text{ W m}^{-2}$  for TOA fluxes and atmospheric absorption, respectively), consistent with the absence of the SW feedback from ozone absorption in this model configuration. This is in contrast with the coupled chemistry run, which yields an increase in the SW absorption of  $0.71 \text{ W m}^{-2}$ . Therefore, in the coupled chemistry integration, the  $\sim 0.3 \text{ W m}^{-2}$  increase in the atmospheric SW absorption, along with the equivalent reduction in surface downwelling SW radiation, is directly linked to stratospheric ozone, while cloud and tropospheric adjustments play a secondary role.

In addition to the SW fluxes, we have also analyzed the other terms of the surface energy budget. Consistent with the surface warming shown in Fig. 2, the SSI increase leads to a stronger upward longwave (LW) emission from the surface, which is more pronounced in the specified chemistry configuration. However, an increase in the downward LW flux overcompensates the change in the upward LW component, resulting in a net decrease in the LW at low latitudes (Fig. 8a). The net (LW and SW) energy gain at the surface is balanced by an increase in evaporation (Fig. 8b), which is larger in the specified chemistry case. Interestingly, the SSI increase leads to negligible changes in the sensible heat flux (Fig. 8c). This indicates a decrease in the Bowen ratio, which is in agreement with the response to solar forcing reported in simpler models (Wetherald and Manabe 1975). Thus, enhanced surface SW absorption over the ocean leads to warmer sea surface temperatures and stronger evaporation. This is balanced by an increase in climatological maxima of tropical precipitation, such as in the warm pool region (Fig. 4), in agreement with the bottom-up mechanism (Meehl et al. 2003, 2009).

The presence of an interactive chemistry in the model thus leads to a decrease in evaporation, and in tropospheric specific humidity, which, in relative terms, maximizes in the upper tropical troposphere at 10 km (see Fig. 9). Interestingly, the opposite effect (an increase in water vapor) is seen in the stratosphere; this is due to a warming of the tropical tropopause layer, resulting in less dehydration and therefore increased stratospheric water vapor concentrations relative to the

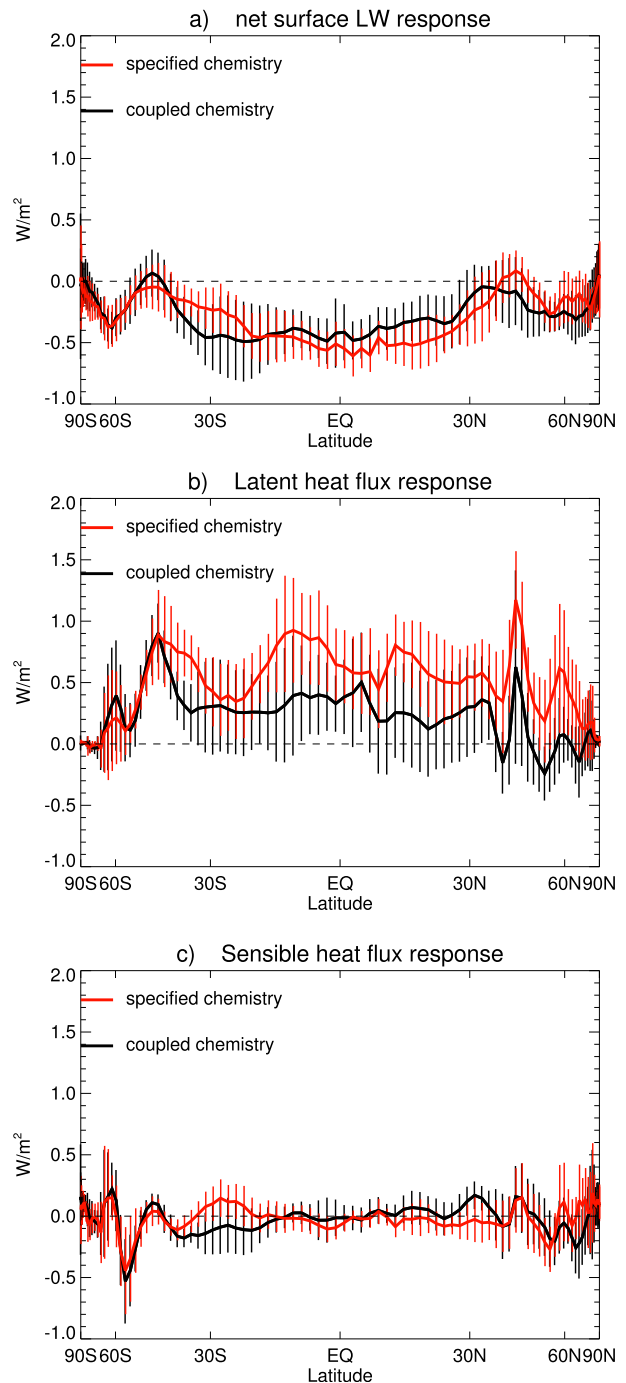


FIG. 8. As in Fig. 3, but for the (a) net surface LW flux and (b) latent and (c) sensible heat fluxes. Units:  $\text{W m}^{-2}$ . All fluxes are positive upward.

specified chemistry integration. An increase in stratospheric water vapor concentrations leads to a positive (LW) radiative forcing at the tropopause (Forster and Shine 2002; Solomon et al. 2010; Dessler et al. 2013). However, the decrease in tropospheric water vapor

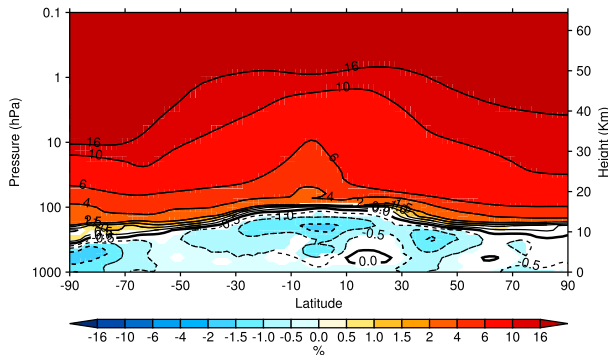


FIG. 9. Contribution of the chemistry coupling to the zonal mean specific humidity response, quantified as the (ctrl4W – ctrl4W\_nochem) difference. Colored areas denote statistically significant differences at the 95% confidence level. Units: %.

overcompensates the positive LW forcing from stratospheric water vapor, as indicated by the decrease in downwelling LW flux at the surface. Since the upper tropospheric moisture is efficient at triggering the water vapor LW feedback (Held and Soden 2000), it is likely that changes in this field arising from the chemistry coupling amplify the differences in the modeled surface response.

In summary, the UV-driven stratospheric ozone increase in the coupled chemistry configuration leads to an increase in stratospheric (and a decrease in surface) absorption of SW radiation. As tropospheric moisture is closely tied to surface temperature (via the Clausius–Clayperon relation), changes in surface SW heating lead to differences in tropospheric water vapor concentrations. Through the water vapor feedback (LW), small changes in tropospheric moisture further amplify the difference between coupled and specified chemistry responses, possibly contributing to the reduction of the model sensitivity to increased SSI by stratospheric ozone.

#### 4. Conclusions

We have investigated the impact of the interactive chemistry on the WACCM model sensitivity to an idealized solar forcing. The main results are as follows:

- The steady-state surface temperature response to an increase in solar irradiance, which we have chosen to be larger than the peak-to-trough variation over the 11-yr solar cycle, resembles the global warming pattern associated with well-mixed GHGs. The broad features are an amplified warming over land and a polar amplification in the Northern Hemisphere (NH).
- The model shows a significantly weaker (by one-third) surface response when ozone is computed interactively and is allowed to respond to solar forcing, as compared to an experiment with fixed ozone. The reduction in the

model sensitivity can be as high as the signal itself, such as in NH high latitudes.

- The smaller surface response in the integrations with interactive chemistry is caused by a UV-induced stratospheric ozone increase, which reduces the absorbed solar radiation at the surface, and hence the efficiency of the “bottom-up” mechanism (Meehl et al. 2009). This results in less evaporation, weaker tropical precipitation response, and through the water vapor (longwave) feedback, the warming within the troposphere is further reduced, as compared to a configuration without an interactive chemistry.

To put our results in a broader context, we note that the mechanism whereby the interactive ozone chemistry reduces climate sensitivity to solar forcing is fundamentally different from the one recently documented by Nowack et al. (2014) for the case of increased CO<sub>2</sub>. In model experiments forced with a quadrupling of CO<sub>2</sub>, they found a global mean surface temperature increase to be 20% smaller in the presence of coupled chemistry (see their Fig. 1). In their study, the reduced climate sensitivity was primarily attributed to a LW effect, owing to ozone and water vapor changes in the tropical lower stratosphere induced by a strengthening of the Brewer–Dobson circulation (BDC). In our experiments, the BDC does not accelerate in response to SSI increases, and ozone changes are largely caused by enhanced oxygen photolysis in the stratosphere, yielding a (negative) surface SW forcing. Hence, while the presence of an interactive ozone chemistry reduces the modeled sensitivity to both GHG and solar forcing, the physical mechanisms appear to be quite different.

Needless to say, the precise amplitude of the impact of coupled chemistry on climate sensitivity is likely to be model dependent. This is due to the role of the LW moisture feedback, whose magnitude varies between models [see, e.g., Fig. 1 in Soden and Held (2006)]. Another factor controlling the amplitude of the impact of coupled chemistry is the spectral distribution of the imposed SSI forcing. A stronger UV forcing, such as that observed in the SORCE satellite data (Ermolli et al. 2013), would induce a different vertical distribution of the stratospheric ozone response (Haigh et al. 2010) and, through changes in column-integrated ozone, of the amount of clear-sky SW absorption. Therefore, the effect of the coupled chemistry on the model sensitivity need not necessarily scale linearly with the imposed UV perturbation. However, the present results are based on a SSI forcing dataset [i.e., the NRL-SSI from Wang et al. (2005)], which is widely used among CMIP5 models (Mitchell et al. 2015). A precise quantification of the model and forcing dependency of this feedback could be addressed in future studies.

Our results suggest a potential overestimate of the surface response to solar forcing in studies based on models that do not employ interactive chemistry. This would be of crucial importance, in particular for simulations of the climate of the last millennium and in many geoengineering studies, where most models often do not account for ozone variability consistent with changes in solar irradiance, which are larger than the 11-yr solar cycle. For these and possibly other applications, it may be prohibitive to perform long model integrations with both a well-resolved stratospheric circulation and interactive ozone chemistry, given the computational limitations. However, as we have shown here, modeling interactive chemistry may not be needed: it might suffice to specify ozone changes that are consistent with the SSI forcing, as was done by the “semi-interactive” coupled chemistry simulation performed by some of the CMIP5 models (Eyring et al. 2013). This entails a considerable computational saving. Our study, therefore, highlights the importance of producing accurate solar-forcing-consistent ozone datasets to be used for future climate model simulations.

*Acknowledgments.* All model integrations were performed at the National Center for Atmospheric Research (NCAR), which is sponsored by the U.S. NSF. The authors thank Michael Previdi, Arlene Fiore, and Luke Valin for their insightful comments on the early draft of this manuscript. We also acknowledge Daniel R. Marsh for his discussions and private communications.

#### REFERENCES

- Ammann, C. M., F. Joos, D. S. Schimel, B. L. Otto-Bliesner, and R. A. Tomas, 2007: Solar influence on climate during the past millennium: Results from transient simulations with the NCAR Climate System Model. *Proc. Natl. Acad. Sci. USA*, **104**, 3713–3718, doi:10.1073/pnas.0605064103.
- Andrews, T., P. M. Forster, O. Boucher, N. Bellouin, and A. Jones, 2010: Precipitation, radiative forcing and global temperature change. *Geophys. Res. Lett.*, **37**, L14701, doi:10.1029/2010GL043991.
- Chiodo, G., N. Calvo, D. Marsh, and R. Garcia-Herrera, 2012: The 11 year solar cycle signal in transient simulations from the Whole Atmosphere Community Climate Model. *J. Geophys. Res.*, **117**, D06109, doi:10.1029/2011JD016393.
- Conley, A., J. Lamarque, F. Vitt, W. Collins, and J. Kiehl, 2012: PORT, a CESM tool for the diagnosis of radiative forcing. *Geosci. Model Dev.*, **6**, 469–476, doi:10.5194/gmd-6-469-2013.
- Cubasch, U., G. Hegerl, R. Voss, J. Waszkewitz, and T. Crowley, 1997: Simulation of the influence of solar radiation variations on the global climate with an ocean–atmosphere general circulation model. *Climate Dyn.*, **13**, 757–767, doi:10.1007/s003820050196.
- Dessler, A., M. Schoeberl, T. Wang, S. Davis, and K. Rosenlof, 2013: Stratospheric water vapor feedback. *Proc. Nat. Acad. Sci. USA*, **110**, 18 087–18 091, doi:10.1073/pnas.1310344110.
- Dietmüller, S., M. Ponater, and R. Sausen, 2014: Interactive ozone induces a negative feedback in CO<sub>2</sub>-driven climate change simulations. *J. Geophys. Res. Atmos.*, **119**, 1796–1805, doi:10.1002/2013JD020575.
- Ermolli, I., and Coauthors, 2013: Recent variability of the solar spectral irradiance and its impact on climate modelling. *Atmos. Chem. Phys.*, **13**, 3945–3977, doi:10.5194/acp-13-3945-2013.
- Eyring, V., T. G. Shepherd, and D. W. Waugh, Eds., 2010: SPARC report on the evaluation of chemistry–climate models. SPARC Rep. 5, WCRP-132, WMO/TD-No. 1526, 434 pp. [Available online at [http://www.atmos.physics.utoronto.ca/SPARC/ccmval\\_final/](http://www.atmos.physics.utoronto.ca/SPARC/ccmval_final/).]
- , and Coauthors, 2013: Long-term ozone changes and associated climate impacts in CMIP5 simulations. *J. Geophys. Res. Atmos.*, **118**, 5029–5060, doi:10.1002/jgrd.50316.
- Fernández-Donado, L., and Coauthors, 2013: Large-scale temperature response to external forcing in simulations and reconstructions of the last millennium. *Climate Past*, **9**, 393–421, doi:10.5194/cp-9-393-2013.
- Forster, P., and K. Shine, 2002: Assessing the climate impact of trends in stratospheric water vapor. *Geophys. Res. Lett.*, **29**, 1086, doi:10.1029/2001GL013909.
- Fröhlich, C., and J. Lean, 2004: Solar radiative output and its variability: Evidence and mechanisms. *Astron. Astrophys. Rev.*, **12**, 273–320, doi:10.1007/s00159-004-0024-1.
- Gent, P. R., and Coauthors, 2011: The Community Climate System Model version 4. *J. Climate*, **24**, 4973–4991, doi:10.1175/2011JCLI4083.1.
- Gillett, N., J. Scinocca, D. Plummer, and M. Reader, 2009: Sensitivity of climate to dynamically-consistent zonal asymmetries in ozone. *Geophys. Res. Lett.*, **36**, L10809, doi:10.1029/2009GL037246.
- Goody, R. M., and Y. L. Yung, 1989: *Atmospheric Radiation: Theoretical Basis*. 2nd ed. Oxford University Press, 544 pp.
- Gray, L., and Coauthors, 2010: Solar influences on climate. *Rev. Geophys.*, **48**, RG4001, doi:10.1029/2009RG000282.
- Haigh, J. D., 1994: The role of stratospheric ozone in modulating the solar radiative forcing of climate. *Nature*, **370**, 544–546, doi:10.1038/370544a0.
- , 1996: The impact of solar variability on climate. *Science*, **272**, 981–984, doi:10.1126/science.272.5264.981.
- , A. R. Winning, R. Toumi, and J. W. Harder, 2010: An influence of solar spectral variations on radiative forcing of climate. *Nature*, **467**, 696–699, doi:10.1038/nature09426.
- Hansen, J. D., and Coauthors, 2005: Efficacy of climate forcings. *J. Geophys. Res.*, **110**, D18104, doi:10.1029/2005JD005776.
- Harder, J. W., J. M. Fontenla, P. Pilewskie, E. C. Richard, and T. N. Woods, 2009: Trends in solar spectral irradiance variability in the visible and infrared. *Geophys. Res. Lett.*, **36**, L07801, doi:10.1029/2008GL036797.
- Hegerl, G., J. Luterbacher, F. González-Rouco, S. F. Tett, T. Crowley, and E. Xoplaki, 2011: Influence of human and natural forcing on European seasonal temperatures. *Nat. Geosci.*, **4**, 99–103, doi:10.1038/ngeo1057.
- Held, I. M., and B. J. Soden, 2000: Water vapor feedback and global warming. *Annu. Rev. Energy Environ.*, **25**, 441–475, doi:10.1146/annurev.energy.25.1.441.
- Huneus, N., and Coauthors, 2014: Forcings and feedbacks in the GeoMIP ensemble for a reduction in solar irradiance and increase in CO<sub>2</sub>. *J. Geophys. Res.*, **119**, 5226–5239, doi:10.1002/2013JD021110.
- Ineson, S., A. A. Scaife, J. R. Knight, J. C. Manners, N. J. Dunstone, L. J. Gray, and J. D. Haigh, 2011: Solar forcing of winter

- climate variability in the Northern Hemisphere. *Nat. Geosci.*, **4**, 753–757, doi:10.1038/ngeo1282.
- Kinnison, D., and Coauthors, 2007: Sensitivity of chemical tracers to meteorological parameters in the MOZART-3 chemical transport model. *J. Geophys. Res.*, **112**, D20302, doi:10.1029/2006JD007879.
- Kleidon, A., and M. Renner, 2013: A simple explanation for the sensitivity of the hydrologic cycle to surface temperature and solar radiation and its implications for global climate change. *Earth Syst. Dyn.*, **4**, 455–465, doi:10.5194/esd-4-455-2013.
- Lee, J. N., D. T. Shindell, and S. Hameed, 2009: The influence of solar forcing on tropical circulation. *J. Climate*, **22**, 5870–5885, doi:10.1175/2009JCLI2670.1.
- Marsh, D. R., R. Garcia, D. Kinnison, B. Boville, F. Sassi, S. Solomon, and K. Matthes, 2007: Modeling the whole atmosphere response to solar cycle changes in radiative and geomagnetic forcing. *J. Geophys. Res.*, **112**, D23306, doi:10.1029/2006JD008306.
- , M. J. Mills, D. E. Kinnison, J.-F. Lamarque, N. Calvo, and L. M. Polvani, 2013: Climate change from 1850 to 2005 simulated in CESM1 (WACCM). *J. Climate*, **26**, 7372–7391, doi:10.1175/JCLI-D-12-00558.1.
- Meehl, G. A., W. M. Washington, T. Wigley, J. M. Arblaster, and A. Dai, 2003: Solar and greenhouse gas forcing and climate response in the twentieth century. *J. Climate*, **16**, 426–444, doi:10.1175/1520-0442(2003)016<0426:SAGGFA>2.0.CO;2.
- , J. M. Arblaster, G. Branstator, and H. van Loon, 2008: A coupled air–sea response mechanism to solar forcing in the Pacific region. *J. Climate*, **21**, 2883–2897, doi:10.1175/2007JCLI1776.1.
- , —, K. Matthes, F. Sassi, and H. van Loon, 2009: Amplifying the Pacific climate system response to a small 11-year solar cycle forcing. *Science*, **325**, 1114–1118, doi:10.1126/science.1172872.
- Merkel, A. W., J. W. Harder, D. R. Marsh, A. K. Smith, J. M. Fontenla, and T. N. Woods, 2011: The impact of solar spectral irradiance variability on middle atmospheric ozone. *Geophys. Res. Lett.*, **38**, L13802, doi:10.1029/2011GL047561.
- Mitchell, D., and Coauthors, 2015: Solar signals in CMIP-5 simulations: The stratospheric pathway. *Quart. J. Roy. Meteor. Soc.*, **141**, 2390–2403, doi:10.1002/qj.2530.
- Myhre, G., and Coauthors, 2014: Anthropogenic and natural radiative forcing. *Climate Change 2013: The Physical Science Basis*. T. Stocker et al., Eds., Cambridge University Press, 659–740.
- Neely, R., D. Marsh, K. Smith, S. Davis, and L. Polvani, 2014: Biases in Southern Hemisphere climate trends induced by coarsely specifying the temporal resolution of stratospheric ozone. *Geophys. Res. Lett.*, **41**, 8602–8610, doi:10.1002/2014GL061627.
- Nowack, P. J., N. L. Abraham, A. C. Maycock, P. Braesicke, J. M. Gregory, M. M. Joshi, A. Osprey, and J. A. Pyle, 2014: A large ozone-circulation feedback and its implications for global warming assessments. *Nat. Climate Change*, **5**, 41–45, doi:10.1038/nclimate2451.
- Peck, E., C. Randall, V. Harvey, and D. Marsh, 2015: Simulated solar cycle effects on the middle atmosphere: WACCM3 versus WACCM4. *J. Adv. Model. Earth Syst.*, **7**, 806–822, doi:10.1002/2014MS000387.
- Previdi, M., and L. M. Polvani, 2014: Climate system response to stratospheric ozone depletion and recovery. *Quart. J. Roy. Meteor. Soc.*, **140**, 2401–2419, doi:10.1002/qj.2330.
- Randel, W., and F. Wu, 2007: A stratospheric ozone profile data set for 1979–2005: Variability, trends, and comparisons with column ozone data. *J. Geophys. Res.*, **112**, D06313, doi:10.1029/2006JD007339.
- Schmidt, G., and Coauthors, 2012: Climate forcing reconstructions for use in PMIP simulations of the last millennium (v1.1). *Geosci. Model Dev.*, **5**, 185–191, doi:10.5194/gmd-5-185-2012.
- Schmidt, H., and Coauthors, 2012: Solar irradiance reduction to counteract radiative forcing from a quadrupling of CO<sub>2</sub>: Climate responses simulated by four Earth system models. *Earth Syst. Dyn.*, **3**, 63–78, doi:10.5194/esd-3-63-2012.
- Sherwood, S. C., S. Bony, and J.-L. Dufresne, 2014: Spread in model climate sensitivity traced to atmospheric convective mixing. *Nature*, **505**, 37–42, doi:10.1038/nature12829.
- Shindell, D. T., D. Rind, N. Balachandran, J. Lean, and P. Lonergan, 1999: Solar cycle variability, ozone, and climate. *Science*, **284**, 305–308, doi:10.1126/science.284.5412.305.
- , G. Faluvegi, R. L. Miller, G. A. Schmidt, J. E. Hansen, and S. Sun, 2006: Solar and anthropogenic forcing of tropical hydrology. *Geophys. Res. Lett.*, **33**, L24706, doi:10.1029/2006GL027468.
- Smith, K., R. Neely, D. Marsh, and L. Polvani, 2014: The Specified Chemistry Whole Atmosphere Community Climate Model (SC-WACCM). *J. Adv. Model. Earth Syst.*, **6**, 883–901, doi:10.1002/2014MS000346.
- Soden, B. J., and I. M. Held, 2006: An assessment of climate feedbacks in coupled ocean–atmosphere models. *J. Climate*, **19**, 3354–3360, doi:10.1175/JCLI3799.1.
- Solomon, S., K. H. Rosenlof, R. W. Portmann, J. S. Daniel, S. M. Davis, T. J. Sanford, and G.-K. Plattner, 2010: Contributions of stratospheric water vapor to decadal changes in the rate of global warming. *Science*, **327**, 1219–1223, doi:10.1126/science.1182488.
- Soukharev, B., and L. Hood, 2006: Solar cycle variation of stratospheric ozone: Multiple regression analysis of long-term satellite data sets and comparisons with models. *J. Geophys. Res.*, **111**, D20314, doi:10.1029/2006JD007107.
- Thompson, D. W., S. Solomon, P. J. Kushner, M. H. England, K. M. Grise, and D. J. Karoly, 2011: Signatures of the Antarctic ozone hole in Southern Hemisphere surface climate change. *Nat. Geosci.*, **4**, 741–749, doi:10.1038/ngeo1296.
- Tilmes, S., and Coauthors, 2013: The hydrological impact of geoengineering in the Geoengineering Model Intercomparison Project (GeoMIP). *J. Geophys. Res. Atmos.*, **118**, 11 036–11 058, doi:10.1002/jgrd.50868.
- Wang, Y.-M., J. Lean, and N. Sheeley Jr., 2005: Modeling the sun’s magnetic field and irradiance since 1713. *Astrophys. J.*, **625**, 522, doi:10.1086/429689.
- Waugh, D., L. Oman, P. Newman, R. Stolarski, S. Pawson, J. Nielsen, and J. Perlwitz, 2009: Effect of zonal asymmetries in stratospheric ozone on simulated Southern Hemisphere climate trends. *Geophys. Res. Lett.*, **36**, L18701, doi:10.1029/2009GL040419.
- Wetherald, R. T., and S. Manabe, 1975: The effects of changing the solar constant on the climate of a general circulation model. *J. Atmos. Sci.*, **32**, 2044–2059, doi:10.1175/1520-0469(1975)032<2044:TEOCTS>2.0.CO;2.
- White, W. B., J. Lean, D. R. Cayan, and M. D. Dettinger, 1997: Response of global upper ocean temperature to changing solar irradiance. *J. Geophys. Res.*, **102**, 3255–3266, doi:10.1029/96JC03549.